Tissue Engineering

Cytoskeletal Changes of Mesenchymal Stem Cells During Differentiation

Gregory Yourek,* Mohammad A. Hussain,† and Jeremy J. Mao‡

Mesenchymal stem cells (MSCs) are progenitors for tissues such as bone and cartilage. In this report, the actin cytoskeleton and nanomechanobiology of human mesenchymal stem cells (hMSCs) were studied using fluorescence microscopy and atomic force microscopy (AFM). Human MSCs were differentiated into chondrocytes and osteoblasts as per previous approaches. Cytochalasin D (CytD) was used to temporarily disrupt cytoskeleton in hMSCs, hMSC-chondrocytes (hMSC-Cys) and hMSC-osteoblasts (hMSC-Obs). Fluorescence microscopy revealed a dose-dependent response to CytD. Removal of CytD from the media of cytoskeleton-disrupted cells led to the recovery of the cytoskeletal structures, as confirmed by both fluorescence microscopy and AFM. Force-volume imaging by AFM evaluated the nanomechanics of all three cell types before, during, and after CytD treatment. Cytochalasin D disruption of cytoskeleton had marked effects on hMSCs and hMSC-Cys, in comparison with limited cytoskeleton disruption in hMSC-Obs, as confirmed qualitatively by fluorescence microscopy and quantitatively by AFM. Treatment with CytD resulted in morphology changes of all cell types, with significant decreases in the observed Young's Moduli of hMSCs and hMSC-Cys. These data suggest human mesenchymal stem cells alter their cytoskeletal components during differentiation. Additional studies will address the mechanisms of cytoskeletal changes using biochemical and biophysical methods. *ASAIO Journal* 2007; 53:●●●–●●●.

Mesenchymal stem cells (MSCs) are self-renewing and multipotential cells with the capacity to differentiate into several distinct end-stage cell lineages that form bone, cartilage, adipose, tendon, muscle, neural, and other connective tissues.[1–6] There is much interest in the potential of MSCs in tissue engineering of bone and cartilage for the treatment of musculoskeletal trauma and disease. Adult MSCs offer certain advantages over embryonic stem cells, including their readiness and availability, because they can be obtained from the same individual.[7] Since their first description,[8] MSCs have been shown to possess remarkable capacity for self-replication[4] and multilineage differentiation capacity. They can be differentiated into bone- and cartilage-forming cells in the presence of chemical supplements and/or bioactive factors.[3,9] Potential applications of MSCs towards regeneration and treatment have been reported, such as for tissue-engineered mandibular condyle,[10] total jaw,[11] osteogenesis imperfecta,[12] cardiac regeneration,[13] metachromatic leukodystrophy, and Hurler syndrome.[14] It has been proposed that the cytoskeleton may play a role in the differentiation of MSCs.[15]

The cytoskeleton plays important roles in cell morphology, adhesion, growth, and signaling. Changes in the cytoskeleton of the cell allow the cell to migrate, divide, and maintain its shape,[16] and the cytoskeleton responds to external mechanical stimuli.[17] The cytoskeleton consists of three components: actin filaments, intermediate filaments, and microtubules. The backbone of the cytoskeleton is F-actin, which clusters to form actin filaments. Filaments can be bundled and crosslinked by several actin-binding proteins in a network and are most likely anchored to stable structures, or anchor sites, in the cell (such as the plasma membrane).[18] The actin network plays a major role in the determination of the mechanical properties of living cells[19,20] by forming a direct link between the integrins and the nucleus, which mechanically stiffens the nucleus and holds it in place.[21]

The atomic force microscope (AFM) was developed in 1986 by modifying the scanning tunneling microscope.[22] Since the early use of AFM for imaging living cells, the subsurface cytoskeletal structures have been observed and described in the nanometer-scale range.[23,24] The portion of the cytoskeleton most readily resolved by the AFM is actin filaments.[25] The conjunction of the AFM with other imaging techniques has also confirmed the ability to study microtubules and intermediate filaments with the AFM.[26,27] It has been demonstrated that tightly adherent cells are stiffer than cells that are loosely attached,[28] suggesting a dynamic reorganization of the cytoskeletal elements is induced by the cellular attachment to the substrate. Upon study of the three cytoskeletal elements with immunofluorescent dyes using confocal laser scanning microscopy, the elasticity of the cell membrane was found to be related to the distribution of the actin and intermediate filaments, but much less to the microtubules.[26] Similar observations in two fibroblast cell lines confirmed the crucial importance of the actin filament network for the mechanical stability of living

From the *Department of Physiology and Biophysics, University of Illinois at Chicago, Chicago, Illinois; †Department of Biotechnology, P.A. College of Engineering, Mangalore, India; and ‡College of Dental Medicine, Columbia University, New York, New York.

Submitted for consideration August 2006; accepted for publication in revised form October 2006.

This study was made possible by grants DE15391 and EB02332 from the National Institutes of Health (to J.J.M.).

Presented in part at the 52nd Annual ASAIO Conference, June 8–10, 2006, in Chicago, Illinois.

Reprint requests: Jeremy J. Mao, DDS, PhD, Columbia University Medical Center, 630 West 168 Street - PH7 East - CDM, New York, NY 10032.

DOI: 10.1097/MAT.0b013e31802deb2d

cells.[19] The disruption of actin filaments causes a decrease in the average elastic modulus of the cell membrane, induced disassembly of microtubules has little effect on cell membrane elasticity.[19]

Although the biochemical events that occur upon stem cell differentiation are well-characterized, there is limited knowledge of the nanocharacteristics of undifferentiated and differentiating human mesenchymal stem cells (hMSCs). We have recently characterized the Young's Modulus and surface roughness of differentiating hMSCs (Patel *et al.*, in preparation); however, how these characteristics relate to the underlying actin cytoskeleton of these cells is unknown. The physical characteristics of a cell have proven to be valuable features of cells; different types of cells have evident variations. We have chosen to focus on Young's Modulus because of the significant differences between undifferentiating and differentiating MSCs found in our laboratory (Patel *et al.*, in preparation).

AQ: 1

The hypothesis of this study was that structural changes associated with human MSC differentiation are actin-cytoskeleton dependent. There are numerous reports of gene expression and protein modifications of hMSCs, and of changes in morphology as differentiation occurs; however, little is known about how the structural aspects of these cells are modified as a result of differentiation. We investigated changes in cytoskeletal and nanomechanical characteristics of hMSCs after differentiation using fluorescence and atomic force microscopy techniques, respectively, in combination with cytoskeletal perturbation.

Materials and Methods

Cell Isolation and Culture

Human mesenchymal stem cells were isolated from commercially available whole bone marrow (AllCells, Berkeley, CA) using RosetteSep (StemCell Technologies, Vancouver, BC) according to the manufacturer's instructions. The RosetteSep antibody cocktail crosslinks unwanted cells in the bone marrow to multiple red blood cells, forming "immunorosettes" that increase the density of the unwanted cells. The hMSCs are not labeled with antibody, so they can be collected as a highly enriched population at the interface between the plasma and the buoyant density medium. Briefly, bone marrow was mixed with phosphate-buffered saline (PBS; Cambrex, East Rutherford, NJ) containing 2% fetal bovine serum (FBS; Atlanta Biologicals, Norcross, GA) and 1 mM EDTA solution. This solution was gently layered on Ficoll-Paque (StemCell Technologies). The solution was centrifuged and enriched cells were removed and centrifuged to separate cells.

The cells were counted and plated at 6.7–13.3 $\times$ 10^3 cells/cm^2 in basal culture media, which was Dulbecco's Modified Eagle's Medium, low glucose (DMEM-LG; Sigma, St. Louis, MO), 1% antibiotic (containing 10 units/l penicillin G sodium, 10 mg/ml streptomycin sulfate, 0.25 mg/ml amphotericin B (Gibco, Invitrogen Corporation, Carlsbad, CA), and 10% FBS. Media was changed every 2 days until cells became confluent. At cell confluence, cells were trypsinized, centrifuged, resuspended in media or freezing solution, and passaged 1:4 or frozen until use, respectively. At passaging, cells were plated in tissue-culture flasks and incubated in 5% CO_2 at 37°C, with fresh media changes every 3 or 4 days.

Cell Differentiation

Osteogenic-supplemented media was basal culture media plus 100 nM dexamethasone, 10 mM β-glycerophosphate, and 50 μg/ml ascorbic acid. Chondrogenic supplemented media was DMEM, high glucose, 1% 1$\times$ ITS+ (BD Biosciences, Franklin Lakes, NJ; containing human recombinant insulin and human transferrin [12.5 mg each], selenious acid [12.5 μg], Bovine Serum Albumin [2.5 g], and linoleic acid [10.7 mg]), 1% antibiotic (containing 10 units/l penicillin G sodium, 10 mg/ml streptomycin sulfate, and 0.25 mg/ml amphotericin B), 100 μg/ml sodium pyruvate, 50 μg/ml ascorbic acid, 40 μg/ml L-proline, 0.1 μM dexamethasone, and 10 ng/ml transforming growth factor-β3. Cells were plated at 1–2 $\times$ 10^3 cells/cm^2 for hMSCs and hMSC-osteoblasts and 5–10 $\times$ 10^3 cells/cm^2 for hMSC-chondrocytes on Thermanox cell culture–treated coverslips. The hMSC-Cys were plated at higher density because of less proliferation in serum-free media so similar confluency for all cell types could be obtained at the time of experimentation. Cells were cultured in unsupplemented and supplemented media for 2 weeks before experimentation.

Actin Staining

Cells were fixed in formaldehyde, permeabilized with Triton X-100, and blocked with 1% BSA. Stock solutions of phalloidin were prepared from Phalloidin-TRITC (Sigma) or "Alexa Fluor" 488 Phalloidin (Molecular Probes) dissolved in DMSO or methanol, respectively. Stock solution was added to 1% BSA in PBS for final concentration of 1 μg phalloidin/1 μl PBS. Cells on coverslips were placed upside down on 25 μl phalloidin solution/1 cm^2 area for 40 minutes at room temperature in dark. Cells were washed with PBS and viewed using Nikon Eclipse E600 or E800 fluorescence microscopes and imaged using Image Pro (Media Cybernetics, Silver Spring, MD) or SPOT (Diagnostic Instruments, Sterling Heights, MI) software.

Actin Disruption

Cytochalasin D (CytD; Sigma) was dissolved in dimethylsulfoxide (DMSO; Fisher; Hampton, NH) for stock solution. Stock solution was added to DMSO to reach CytD concentrations of 0.02, 0.09, 0.4, 2, 9, and 19.7 μM in media. As a vehicle control, the same amount of DMSO was added to the media of cells not receiving CytD. At no point did the concentration of DMSO exceed the manufacturer's recommended concentration (0.1%) so cells would not be adversely affected. Stock solution was diluted in a specific amount of DMSO for each concentration used so that the amount of DMSO added to the media was kept the same throughout all experiments. Cells were exposed to the CytD solutions for 2 and 24 hours, after which the cells were fixed and stained or washed 2$\times$ with PBS and non-CytD respective media was added for an additional 6 hours. After 6 hours, these cells were fixed and stained as well. Cell viability with application of 2 μM CytD in DMSO and 0.1% DMSO in media was analyzed via a TUNEL assay kit (Roche, Mannheim, Germany) according to the manufacturer's instructions. Briefly, cells were fixed and permeabilized as above. For positive control, cells were incubated with DNase I; for negative control, cells were incubated with TUNEL-label instead of TUNEL reaction mixture solution from above. Cells were incubated with TUNEL reaction mixture followed by

incubation with TUNEL-AP. Actin cytoskeleton disruption experiments were repeated a minimum of three times for each cell type using multiple donor cells and passage numbers.

Atomic Force Microscopy

The cells on the disc were attached to a 15 mm metal disc using double-sided tape and magnetically attached to the stage of a Nanoscope IIIa AFM (Digital Instruments Inc., Santa Barbara, CA). To measure Young's Moduli in the force-mapping mode, spatially resolved information was obtained by recording a "force-volume image" consisting of arrays of force-distance curves. Cantilevers with a nominal force constant of k = 0.06 N/m and oxide-sharpened Si_3N_4 tips were used to apply nanoindentation of ~1 nN against cell membrane surface. Scan rates were 1 Hz for topographic imaging and 10 Hz for force spectroscopy and scan size area between 50 and 70 μm^2 for imaging and 100 μm^2 for force spectroscopy. Typically, the force maps were recorded with a frequency of 10 Hz at a resolution of 32 × 32 curves. The radius of curvature of the scanning tips was approximately 20 nm. Both topographic and force spectroscopy images of the cell were obtained in contact mode. A standard AFM fluid cell with the o-ring seal was used to keep the cells in a fluidic environment. Degassed DMEM was infused into the fluid cell of the AFM via a syringe pump at 0.05 ml/min. For each cell, average E was derived from individual calculations of three randomly selected points on the membrane surface within the 100 μm^2 scanning field, using the Hertz equation shown below:

$$E = \frac{3F(1 - \nu)}{4\sqrt{R}\sigma^{3/2}} \quad (1)$$

where E is the Young's Modulus, F is the applied nanomechanical load by the AFM, υ is the Poisson ratio for a given region, R is the radius of the curvature of the AFM tip, and σ is the amount of indentation as measured by the AFM. For cytoskeleton disruption, CytD was added at 1 μg/ml (2 μM) to de-gassed DMEM with no additions and infused into the fluid cell as above. For cytoskeleton rescue, medium not containing CytD was again infused. Young's Modulus AFM experiments were repeated 10 times for each cell type using multiple donor cells and passage numbers. Cytoskeleton AFM experiments were repeated a minimum of three times for each cell type using multiple donor cells and passage numbers.

Statistics

Significance was determined at $p \leq 0.05$. Observed Young's Moduli were analyzed with a one-way analysis of variance between all cell types analyzed both before and after exposure to 1 μg/ml (2 μM) CytD. All statistical analysis was carried out using the SigmaPlot 9.0/SigmaStat 3.1 (Point Richmond, CA) software package.

Results

Fluorescence Microscopy and Cytoskeleton Disruption

Upon differentiation, there were evident differences in the actin cytoskeleton structure between undifferentiated hMSCs (**Figure 1A**) and their bone cell counterparts (hMSC-Obs) (**Figure 1B**). The fibroblast-like, spindle shape of the hMSCs translated into long, thin stress fibers running in parallel according to the orientation of the cells (**Figure 1A**). However, upon differentiation to hMSC-Obs, the parallel fibers disappeared, and a robust, crisscrossed pattern of actin cytoskeleton emerged while the stress fibers appeared thicker (**Figure 1B**).

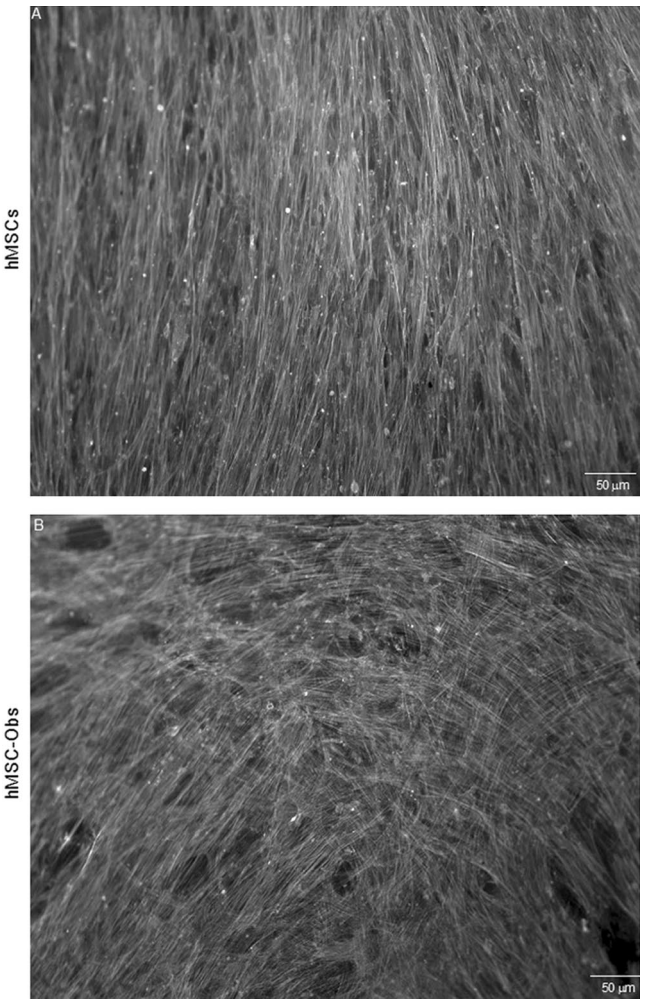

Figure 1. Detailed images of actin cytoskeleton of differentiating hMSCs. Representative images of fluorescently stained actin cytoskeleton of hMSCs (A) and hMSC-Obs (B). Cells were stained with fluorescent phalloidin (which specifically stains cellular F-actin) and images were converted to grayscale where actin is white. Undifferentiated hMSCs displayed long, parallel, thin stress fibers (A). Upon osteogenic differentiation, stress fibers became robust and acquired a crisscross pattern (B).

Human mesenchymal stem cells from multiple donors and passages were culture-expanded in basal (hMSC), osteogenic (hMSC-Obs), and chondrogenic (hMSC-Cys) media for 14 days. Cells were exposed to 0.02, 0.09, 0.4, 2, 9, and 19.7 mM CytD for 2 and 24 hours, as described above. A TUNEL assay demonstrated minimal cell apoptosis of cells exposed to either of these reagents (data not shown) compared with cells not exposed to either of the agents. Therefore, these concentrations were considered acceptable in terms of cell viability for the remaining experiments. Actin cytoskeleton staining revealed a dose-dependent response of actin cytoskeleton of all cell types to CytD. With increasing concentrations of CytD, a greater amount of actin was unable to polymerize, resulting in

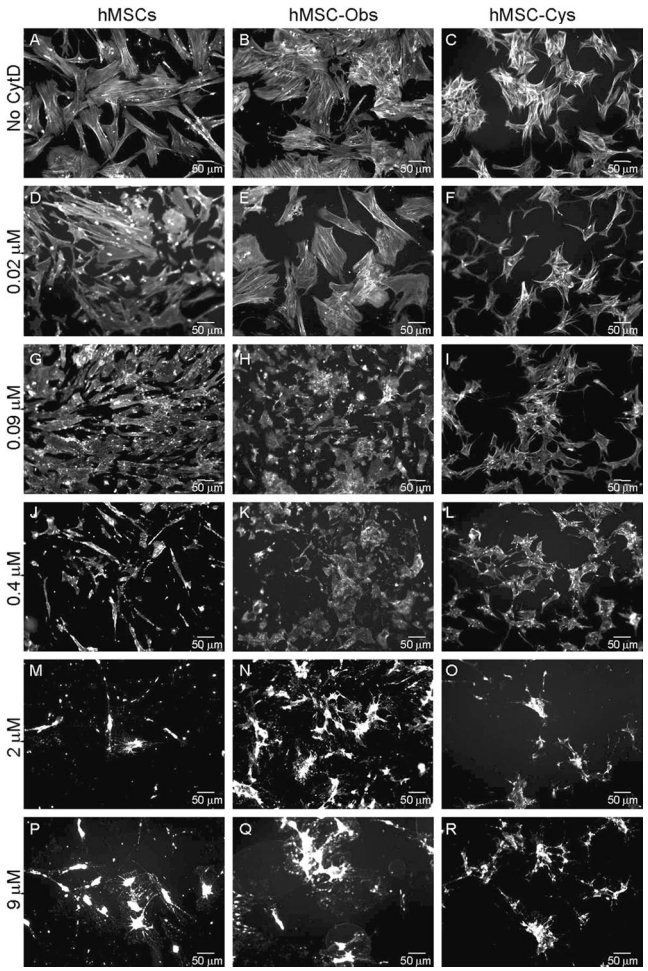

Figure 2. Dose-dependent response of hMSCs to CytD. Representative images of fluorescently stained actin cytoskeleton of hMSCs (A, D, G, J, M, P), hMSC-Obs (B, E, H, K, N, Q), and hMSC-Cys (C, F, I, L, O, R) cells. Cells were in no (A–C), 0.02 μM (D–F), 0.09 μM (G–I), 0.4 μM (J–L), 2 μM (M–O), and 4 μM (P–R) CytD for 2 hours. Cells were stained with fluorescent phalloidin (which specifically stains cellular F-actin) and images were converted to grayscale where actin is white. Extensive cytoskeletal disruption of hMSCs and hMSC-Cys was apparent at and >2 μM CytD. The cytoskeleton of hMSC-Obs appeared robust relative to hMSCs and hMSC-Obs, with seemingly more actin cytoskeleton staining of hMSC-Obs than hMSCs and hMSC-Cys at these concentrations.

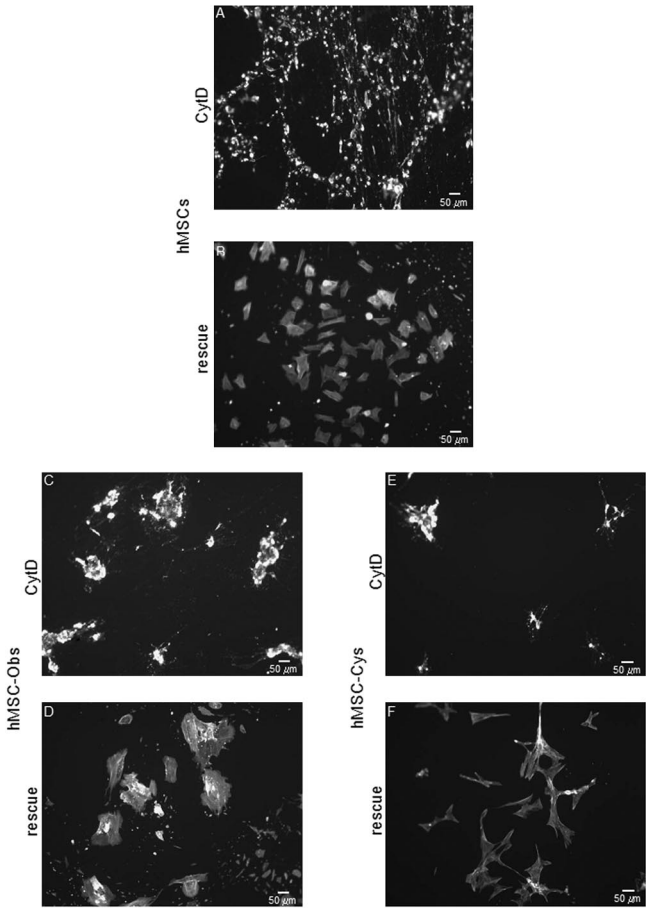

Figure 3. Disruption and rescue of CytD disrupted cells at high CytD concentration. Representative images of fluorescently stained actin cytoskeleton of hMSCs (A, B), hMSC-Obs (C, D), and hMSC-Cys (E, F). Cells were fixed, stained and imaged after 2-hour exposure to 19.7 μM CytD (A, C, E) and rescue after 24-hour exposure to 19.7 μM CytD followed by washing of CytD media and reintroduction of non-CytD respective media for 6 hours (B, D, F). Cells were stained with fluorescent phalloidin (which specifically stains cellular F-actin) and images were converted to grayscale where actin is white. Extensive cytoskeletal disruption of all cells was apparent at this concentration of CytD. All cell types were able to have their cytoskeleton rescued after 24-hour exposure to this CytD concentration followed by a thorough washing and re-application of non-CytD respective media demonstrating no loss of actin polymerization activity or cell viability with the application of the drug.

smaller and more rounded cells (**Figure 2**). A greater effect was seen in hMSCs and hMSC-Cys than in hMSC-Obs, with a greater concentration of CytD necessary for actin disruption/cell rounding in hMSC-Obs than the other cell types (**Figures 2 and 3**, hMSC-Obs images *vs.* hMSCs and hMSC-Cys images). At 2 μM CytD (**Figure 4**) and at the highest concentration of CytD used (19.7 μM) (**Figure 3**), all cell types could have their actin cytoskeleton rescued, even after 24-hour continuous exposure to the drug and only 6-hour re-application of non-CytD media, demonstrating the actin cytoskeleton still possessed polymerization capabilities and cells were still viable after exposure to the CytD and DMSO.

Atomic Force Microscopy: Topography

The hMSCs, hMSC-Obs, and hMSC-Cys were culture-treated in respective media and analyzed using an atomic force microscope. Topographical images were obtained in both height and deflection mode. Scanning in height mode generally revealed a larger height scale of hMSC-Obs than the undifferentiated hMSCs (scale in **Figure 5A** *vs.* **5B**). This was apparently related to the thicker actin stress fibers of the hMSC-Obs than the hMSCs, which could be visualized in detail in deflection mode (noted by arrowheads in **Figures 5B** and **5B′**). In all cell types, scanning in deflection mode revealed the fine cytoskeletal structure (presumably actin) just under the cell membrane at stunning detail (**Figures 5A** and **5B** and **Figure 6A**).

After 1 hour of scanning in basic media, 2 μM CytD was injected via syringe pump into the fluid cell system, which hydrates the cells during AFM studies, while AFM scanning was continued. At this point, the fine cytoskeleton structure began disintegrating. Almost immediately upon introduction of

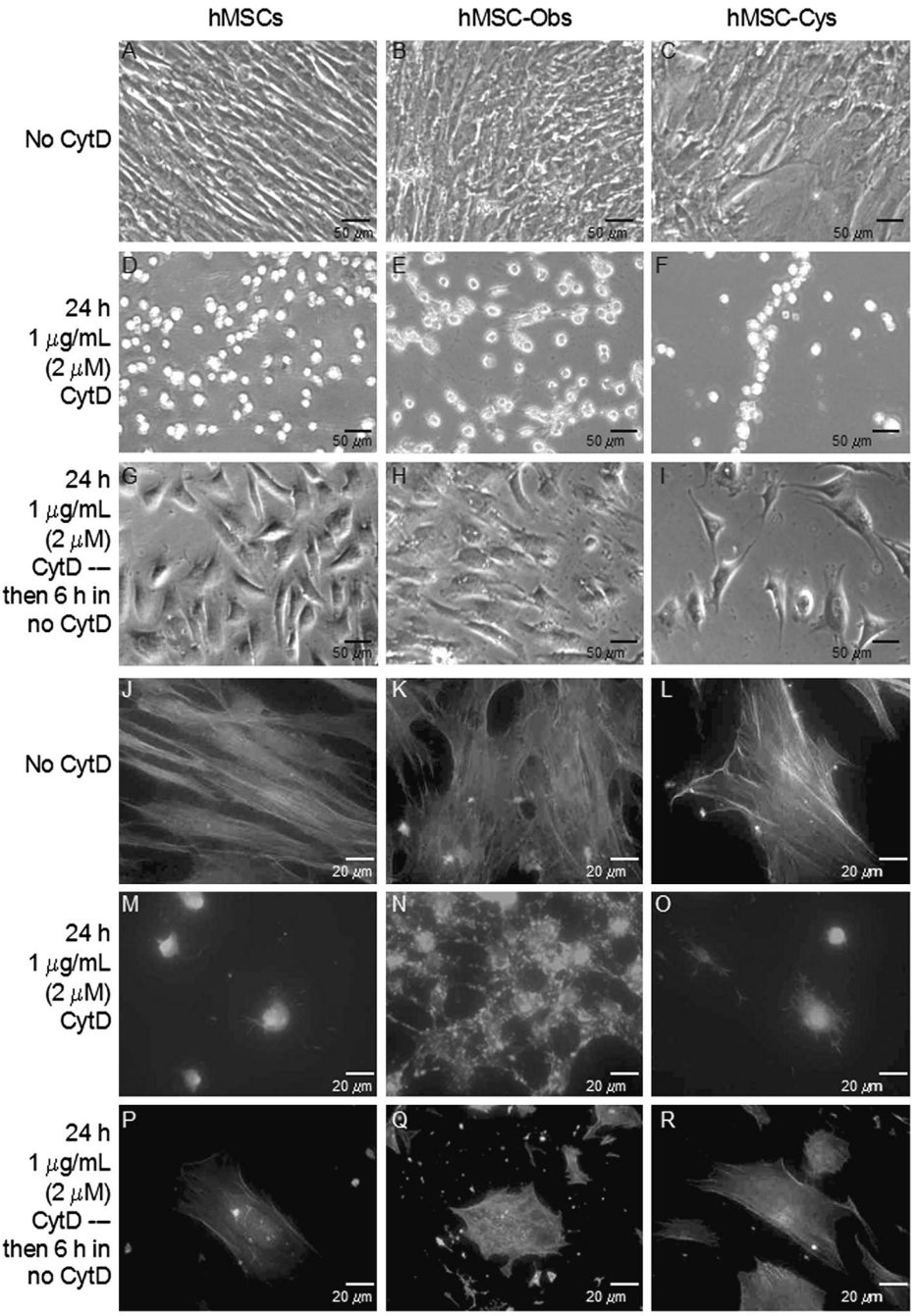

Figure 4. Disruption and rescue of CytD disrupted cells at 1 μg/ml (2 μM) visualized by phase-contrast and fluorescence microscopy. Representative phase-contrast (A–I) and fluorescently stained actin cytoskeleton (J–R) images. Fluorescence images show actin fibers stained with fluorescent phalloidin (which specifically stains cellular F-actin). Images are converted to grayscale where actin is white. Cells were hMSCs (A, D, G, J, M, P), hMSC-Obs (B, E, H, K, N, Q) and hMSC-Cys (C, F, I, L, O, R). Cells were fixed, stained and imaged after culturing without CytD media (A–C, J–L), after 24-hour application of CytD media (D–F, M–O) and rescued after CytD treatment by re-application of non-CytD media for 6 hours (G–I, P–R). All cell types were affected by this concentration of CytD, with more of an effect on hMSCs and hMSC-Cys than on hMSC-Obs (M and O vs. N). All types had F-actin rescued from disruption with removal of CytD, washing and introduction of non-CytD media for 6 hours (P–R). Fewer hMSC-Cys were present during CytD treatment and after rescue because of detachment by CytD treatment (F and I).

drug, the cytoskeleton of all cell types became less pronounced. This effect was much more evident with the application of CytD to hMSCs (**Figures 5A′, 5C′,** and **5E′**) and hMSC-Cys (**Figures 6A′, 6B,** and **6B′**) than to hMSC-Obs (**Figures 5B′, 5D′,** and **5F′**). The greater effect of CytD on the undifferentiated and chondrogenic-differentiated cells compared with the osteogenic-differentiated cells visualized by AFM shadows those images obtained by fluorescent staining (see **Figures 1–3**). After only 10–20 minutes of CytD application, there was a tremendous change in actin cytoskeleton of both the hMSCs and hMSC-Cys. The fine strands of the actin cytoskeleton of the hMSCs disappeared, and the cell mem-

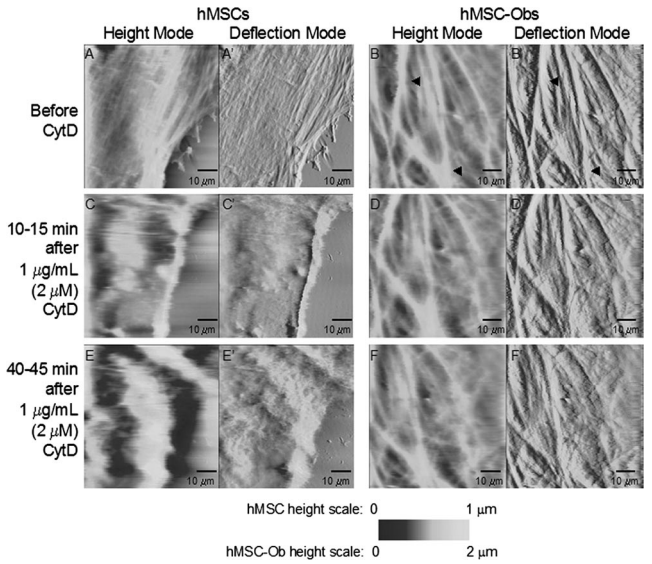

Figure 5. Cytoskeleton disruption of hMSCs and hMSC-Obs visualized by AFM. Representative AFM height (A, B, C, D, E, F) and deflection (A′, B′, C′, D′, E′, F′) scans of hMSCs (A, A′, C, C′, E, E′) and hMSC-Obs (B, B′, D, D′, F, F′). Images of the two cell types before CytD treatment (A,A′,B,B′), after 10–15 minutes of 1 μg/ml (2 mM) CytD exposure (C,C′,D,D′), and after 40–45 minutes of CytD exposure (E,E′,F,F′). In height images, brighter color indicates higher distance off of substrate. Height images of hMSC-Obs generally had a larger z-scale, apparently because of thicker stress fibers that could be visualized just under the surface of the membrane (arrowheads in B and B'). The detailed structure of presumably the actin cytoskeleton could be observed with AFM with both cell types (A′ and B′). There was a marked difference in cytoskeleton morphology of hMSCs exposed to CytD compared with hMSC-Obs (C′ *vs.* D′ and E′ *vs.* F′), with a greater effect of disruption of actin cytoskeleton in hMSCs than in hMSC-Obs.

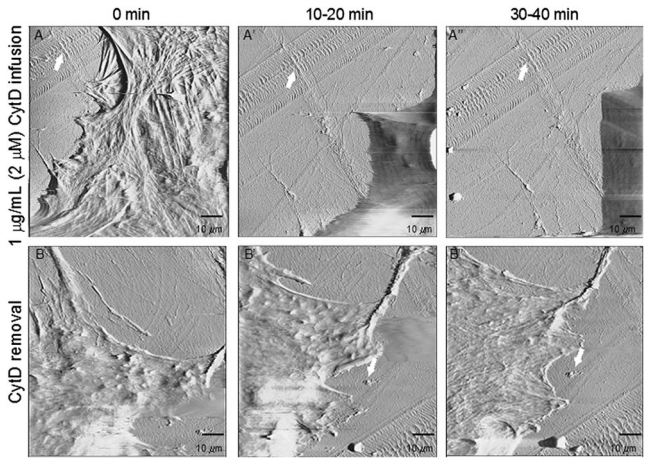

Figure 6. Disruption and rescue of CytD disrupted cells at 1 μg/ml (2 μM) visualized by AFM. Representative AFM deflection images of hMSC-Cys exposed to 1 μg/ml (2 μM) CytD after 10–20 minutes (A′) and 30–40 minutes (A″) of CytD infusion and after 10–20 minutes (B′) and 30–40 minutes (B″) of re-application of non-CytD media. White arrows in A–A″, B′, and B″ denote a landmark to demonstrate a lack of extensive AFM drift. The actin cytoskeleton of hMSC-Cys could be disrupted with exposure to 2 μM CytD. The disruption was so extreme from A–A″ in only a matter of 40 minutes that the cell completely rounded up and left the field of view. In B–B″, a different cell from that seen in A–A″ was re-introduced to non-CytD media after having been exposed to 2 μM CytD media. The actin cytoskeleton can be seen to reform its structure in only 40 minutes, with the cell membrane transforming from a smooth appearance in B to having apparent actin fiber formation visible just under the surface of the cell membrane in B″.

brane became smoother in appearance. In the case of the hMSC-Cys, there was even retraction of the cell after only a short amount of time with CytD; this movement can be assumed to be equal to the rounding up of cells observed in the fluorescent images of cells exposed to higher doses of CytD. However, the thick stress fibers of the hMSC-Obs remained visible by AFM for up to 40 minutes after CytD infusion.

As in the fluorescence studies, rescue of actin cytoskeleton could be noted with AFM scanning (**Figures 6B–B″**). With the removal of the CytD, after only 30–40 minutes of re-application of CytD-free media, the fine structures of the actin cytoskeleton were again visualized just under the cell membrane of hMSC-Cy and the cell began to spread. The landmarks denoted by the arrows in **Figures 6A–A″, 6B,** and **6B′** demonstrate a lack of extensive AFM drift during scanning. This illustrates the disappearance of the cell specifically in **Figures 6 A–A″** is not an artifact due to AFM drift.

Atomic Force Microcopy: Force Spectroscopy

Using force-volume plots, a relative stiffness of the cell membrane can be obtained. With infusion of 2 μM CytD, the relatively definitive point of tip contact with the surface observed in the force-volume plots of the undifferentiated hMSCs transformed to a less defined region, which is evidence of a softening of the membrane most likely due to the disruption of the actin cytoskeleton via CytD (**Figure 7A** *vs.* **7C**). There was a much greater loss of stiffness of hMSCs than hMSC-Obs after introduction of CytD, as the plots before and after CytD introduction to hMSC-Obs (**Figure 7B** vs. **7D**) showed minimal differences. F7

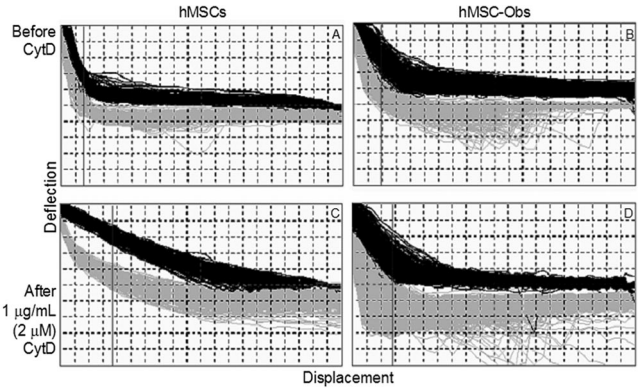

Figure 7. Representative force-volume plots of hMSCs (A,C) and hMSC-Obs (B,D). The y-axis is deflection of the atomic force microscope cantilever/tip and the x-axis is displacement of the cantilever/tip from the surface. Dark lines represent the cantilever/tip approaching the surface; gray lines represent the retraction of the cantilever/tip from the surface. Plots A and B are before the application of actin cytoskeleton disrupting drug CytD, C and D are after application of the drug. The greater angular deviation from A to C as opposed to B to D represents a greater loss of stiffness of hMSCs than hMSC-Obs after the introduction of 1 μg/ml (2 μM) CytD.

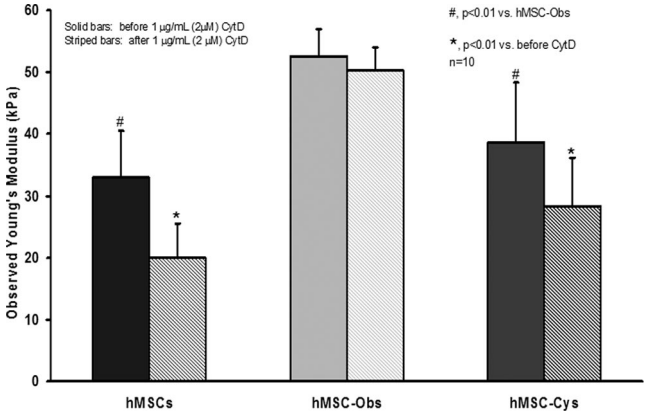

Figure 8. Observed Young's Moduli of hMSCs exposed to CytD obtained by atomic force microscopy. Observed Young's Moduli of hMSCs (black bars), hMSC-Obs (light gray bars), and hMSC-Cys (dark gray bars). Atomic force microscopy measurements were obtained before (solid line bars) and after (striped line bars) application of 1 μg/ml (2 μM) actin cytoskeleton-disrupter CytD. Observed Young's Moduli were obtained from force-volume plots generated by atomic force microscopic nanoindentation of cells in combination with the Hertz model. Bars are means and SEMs of at least 10 separate experiments. Data were analyzed with a one-way analysis of variance. The hMSC-Obs had significantly higher observed Young's Moduli than both hMSCs and hMSC-Cys. Upon actin cytoskeleton disruption, there were significant decreases in the Young's Moduli of both hMSCs and hMSC-Cys; however, no significant decrease was observed for the hMSC-Obs.

More quantitatively, the information from these plots in tandem with the Hertz model can give an observed Young's Modulus of the cell's membrane, which is most likely influenced by the state of the actin cytoskeleton. As we previously found (Patel, *et al.*, in preparation), exposure to osteogenic supplements significantly increased the observed Young's Moduli of hMSC-Obs 0.6-fold compared with the hMSCs in basal media (**Figure 8**). Also, the hMSC-Obs had a significantly higher (0.4-fold) observed Young's Moduli than the hMSC-Cys. Following the addition of 2 μM CytD to the media, the observed Young's Moduli of both the hMSCs significantly decreased 0.4-fold, and the hMSC-Cys significantly decreased 0.3-fold compared with their respective cell type in CytD-free media. However, there was not a significant decrease in the Young's Moduli of hMSC-Obs exposed to 2 μM CytD.

AQ: 2

F8

Discussion

There is a myriad of literature concerning the biochemical changes that occur upon MSC differentiation. However, little is known about the regulation of the actin cytoskeleton of hMSCs upon differentiation. After only 2 weeks' exposure to osteogenic supplements in cell culture medium, the actin cytoskeleton visualized by fluorescence microscopy of hMSC-Obs transforms from an apparently well-organized structure, with fine actin fibers running in parallel along the long axis of the cell of the undifferentiated hMSCs, to a seemingly reorganized and robust arrangement of the actin cytoskeleton in the hMSC-Obs (**Figure 1A** vs. **1B**). This reorganization of the actin cytoskeleton may be related to the responsiveness of the actin cytoskeleton in the response of bone cells to a shear stress,[29,30] which plays a major role in bone modeling/remodeling.[31] Less obvious were the changes in the actin cytoskeleton of the hMSCs differentiating into cartilage cells; there seemed to be an increase in actin-based protrusions emanating from the hMSC-Cys as compared with the hMSCs (**Figure 2A** vs. **2C**), which may also be due to the importance of the actin cytoskeleton in cartilage cells.[32]

By using CytD to inhibit actin polymerization[33] of undifferentiated hMSCs and hMSCs differentiating to bone (hMSC-Obs) and cartilage (hMSC-Cys), we have gained a better understanding of the structural changes an hMSC experiences upon differentiation. The actin cytoskeleton (visualized by way of fluorescently stained actin) of both hMSCs and hMSC-Cys became almost completely disrupted at 2 μM CytD (see **Figures 3M** and **3O**). The observed decrease in the number of cells after disruption and rescue of the actin cytoskeleton are most likely an effect of the complete disruption of the cytoskeleton of many of the cells, which would cause the cell to completely round up and lose contact with the substrate. The following washing of CytD media for re-application of non-CytD media may have washed these cells away. There appear to be fewer hMSC-Cys remaining after rescue than hMSCs and hMSC-Obs (**Figures 4G** and **4H** vs. **4I**). This may be because of a loss of actin cytoskeleton structures during chondrogenic differentiation, as redifferentiated chondrocytes display faint actin microfilaments when compared to their dedifferentiated counterparts.[34]

It has previously been found that the cytoskeleton may affect the differentiation of cells.[35,36] Recently, through disruption of the actin cytoskeleton using CytD, a decrease in the osteogenic markers alkaline phosphatase activity and calcium deposition of human mesenchymal stem cell–derived osteoblasts was noted compared with those cells not exposed to the cytoskeleton disrupting drugs.[15] It was also quite elegantly displayed using micropatterning that hMSCs expressed osteogenic or adipogenic markers depending on the size of the micropattern on which the cells were cultured.[37] When the cells were cultured on patterns with small areas, they exhibited an adipogenic phenotype. Likewise, when the actin cytoskeleton of the cells was disrupted, transforming their normal fibroblast-like, spindle-shaped morphology to a rounded-up cell, adipogenic markers were increased. This was true even when the cells were cultured in the presence of osteogenic-supplemented media in both cases. Conversely, when the cells were allowed to spread on a large pattern, the cells expressed a more osteogenic phenotype. This was found even when the cells were cultured in adipogenic-supplemented media. This differentiation brought about by changes in cell shape was found to be mediated through the RhoA-ROCK pathway.[37] Similar results are reported in this work; when undifferentiated hMSCs are cultured in the presence of osteogenic supplements, their cytoskeleton transforms from long, mostly parallel stress fibers of hMSCs to robust stress fibers with more random patterning of hMSC-Obs (**Figure 1B**). This radical change in the actin cytoskeleton after only 2 weeks may be explained by the idea that the cytoskeleton and its related proteins of bone[29,38] and cartilage[39,40] cells play a role in the mechanotransduction of mechanical signals to which these cells are exposed.

The differences in actin cytoskeleton properties of these cell types may be related to the amount/type of actin capping proteins present in the cells, which have a function in the polymerization of actin filaments. It has been hypothesized that the actions of cytoskeleton-disruption drugs, specifically CytD, depend on the affinity of capping proteins for the barbed

filament ends of cells.[18] A higher concentration of CytD is needed for extensive actin cytoskeleton disruption for cells that have capping proteins with a higher affinity, because the CytD is less able to displace the actin-capping proteins, thus blocking actin polymerization,[18] This may, in part, explain the differences seen in the current work between the amount of CytD necessary for maximum actin disruption among the three cell types. It may be that the MSCs differentiating into bone cells acquire changes in their production of actin-capping proteins along with their changes in cell morphology and increases on bone cell markers. Gelsolin is an example of an actin-capping protein that mediates actin dynamics, thereby modulating cell shape and movement.[41] Gelsolin *in vitro* can become associated with phosphoinositides, which have been shown to regulate actin regulatory proteins.[42] Osteopontin has been shown to upregulate gelsolin-associated phosphoinositides in osteoclasts, which causes uncapping of actin and results in actin filament polymerization.[43] Because an increase in osteopontin production is noted during MSC differentiation to bone cells in some models,[44] this increase in osteopontin may be regulating the activity of gelsolin, thereby modulating actin polymerization/depolymerization. Further work in this area is necessary to determine if this is the case.

Using AFM, we were able to observe actin cytoskeleton disruption and repolymerization of hMSCs and their differentiated counterparts as the events were occurring in the same cell with stunning resolution (**Figures 5** and **6**). With the high-resolution images gained with the AFM, coupled with images obtained using conventional fluorescence microscopy, we can conclude that there are obvious differences in the actin cytoskeleton of undifferentiated and differentiated hMSCs. Undifferentiated hMSCs portray their typical fibroblast-like, spindle-shaped morphology, and the actin cytoskeleton seems to have the responsibility for that particular shape of the cell because the majority of the actin fibers run in parallel down the long axis of the cell. Upon osteogenic differentiation, the actin cytoskeleton becomes robust and more disordered with a greater amount of crisscrossing actin filaments and larger stress fiber bundles. As previously stated, this may have to do with the specific responsibility of the actin cytoskeleton of bone cells to directly aid in the response of bone cells to a shear stress,[29,30] which has been hypothesized as the basis for the modeling/remodeling of the entire skeleton.[31] The actin cytoskeleton of the hMSCs differentiating into cartilage cells also underwent changes, but to a lesser degree. The undifferentiated cells went from their previously described shape to spreading out more with additional actin protrusions, possibly due to the importance of the actin cytoskeleton in cartilage cells.[32] Also with AFM, it was possible to observe the degree to which a single cell responded to the actin cytoskeleton-disrupting drug CytD in near-real time and how a cell responds to the removal of the drug (**Figure 6**). As in the fluorescence microscopy experiments (**Figures 2G** and **2H** vs. **2I**), a higher degree of cell rounding up/detachment of hMSC-Cys as compared with hMSCs and hMSC-Obs (**Figures 5E′** and **5F′** vs. **Figure 6A″**) could also be noted with AFM, so much so that the cell completely leaves the scanning area of the AFM. This is similar to the apparent decrease of hMSC-Cys present after cytoskeleton disruption/rescue visualized by fluorescent staining (**Figure 4I**) and further demonstrates the differences in the cytoskeleton of undifferentiated stem cells and chondrogenic-differentiated stem cells.

The actin cytoskeleton has previously been demonstrated to play a larger role in the nanomechanical properties of cells than the microtubule component.[19] However, most AFM studies take care not to use large loading forces or penetrate the cell too much so as not to damage the cell during scanning. When the nanomechanics of a cell are probed at a level deeper than at the membrane surface, the microtubule network does appear to play a role.[45] Further studies that use possibly better models for Young's Modulus development may be warranted, as may those that study the role of the microtubular portion of the cytoskeleton of undifferentiated and differentiating stem cells. Also, with the disruption of the actin cytoskeleton and sequential rounding up of the cell, AFM force-volume mode may have been biased towards scanning closer to the nucleus, as the bulk of the cell consisting of the actin cytoskeleton has retracted. Other studies using AFM have noted differences in the Young's Moduli at different locations of the cell, specifically between locations near the periphery of the cell compared with locations that were scanned directly on, or in close proximity to, the cell nucleus.[46,47] It would be interesting in a future study to determine the Young's Moduli at different locations of each type of cell before and after actin cytoskeleton disruption to determine if the changes in Young's Moduli associated with actin cytoskeleton disruption may in part be affected by the decrease in total cell surface area available for AFM scanning and an increase in scanning of the membrane of the cell that is just above the nucleus as a result of the retraction of the cell due to CytD exposure.

Using combined approaches of fluorescence microscopy and uniaxial stress-strain testing device, Wakatsuki and others found a correlation between the degree of actin polymerization and the mechanical properties of the cells studied.[18] Interestingly, they observed that, even at lower concentrations of actin-disrupting drugs used when there was no noticeable actin cytoskeleton disruption visualized by fluorescence microscopy, changes were evident in the mechanical properties of these cells. Although the experiments described in this work did not go so far as to test the mechanical properties of all cell types at all CytD concentrations used, some conclusions can be drawn concerning the dependence on hMSC nanomechanics on their associated actin cytoskeleton. At the dose of CytD used for the nanomechanical studies in the current experiment, 2 μM, undifferentiated hMSCs and hMSCs exposed to chondrogenic supplements had a significant decrease in their Young's Moduli, or stiffness, of their cell membrane. This was evident by AFM not only quantitatively via direct measurement of this property, but qualitatively as well with topographical force and deflection mode images of the flattening surface of the cells with CytD infusion and the disruption of the actin cytoskeleton.

Conclusion

Using AFM to measure cell mechanics has recently gained popularity as an important tool for studying how cells respond to specific stimuli. Biological techniques to study changes in cell behavior have been well researched for decades; it is only recently that an understanding of the physical properties of

cells has become essential for eventual therapeutic applications. We attempted to gain a better understanding of the structural transformations a human mesenchymal stem cell goes through upon differentiation to a bone- or cartilage-producing cell. We believe this to be important in the field of stem cell biology because although much is known concerning the biochemical changes a stem cell experiences during differentiation, little is known about the direct physical changes a cell goes through upon differentiation. This may have wide implications in the field of tissue engineering, where structure is as important as chemistry.

We have found that the actin cytoskeleton of mesenchymal stem cells undergoes changes upon osteogenic and chondrogenic differentiation. In the case of osteogenesis, the parallel cytoskeleton with thin actin fibers becomes disordered and robust with thicker stress fibers. In the case of chondrogenesis, the cytoskeleton expands from a parallel orientation to having more projections emanating from the center of the cell. The actin cytoskeleton of hMSC-Obs was also more resistant to drug disruption than was the actin cytoskeleton of hMSCs and hMSC-Cys. The observed Young's Moduli of the hMSC-Obs were higher than both the hMSCs and hMSC-Cys, possibly as a result of the previously described cytoskeleton reorganization. Disruption of actin cytoskeleton and associated AFM studies with more doses of the cytoskeleton disrupter may further describe changes in the structure of the hMSCs. In both cases, these changes in the cytoskeleton may serve to structurally transform the cell so it is able to respond to stimuli experienced by bone and cartilage cells that are necessary for the health of the tissue. Understanding the physical characteristics of these cells may aid in the development of new biomaterials, which can potentiate the structure of the cells for the advancement of tissue engineering.

Acknowledgments

We would like to acknowledge Dr. Susan McCormick for thoughtful insight and assistance with fluorescence microscopy and Dr. Primal de Lanerolle for helpful discussion and critical reading of the manuscript.

References

1. Azizi SA, Stokes D, Augelli BJ: Engraftment and migration of human bone marrow stromal cells implanted in the brains of albino rats: Similarities to astrocyte grafts. *Proc Natl Acad Sci U S A* 95: 3908–3913, 1998.
2. Young RG, Butler DL, Weber W: Use of mesenchymal stem cells in a collagen matrix for Achilles tendon repair. *J Orthop Res* 16: 406–413, 1998.
3. Pittenger MF, Mackay AM, Beck SC, *et al*: Multilineage potential of adult human mesenchymal stem cells. *Science* 284: 143–147, 1999.
4. Alhadlaq A, Mao JJ: Mesenchymal stem cells: Isolation and therapeutics. *Stem Cells Dev* 13: 436–448, 2004.
5. Marion NW, Mao JJ: Mesenchymal stem cells and tissue engineering, in Lanza R, Klimanskaya I (eds), *Methods in Enzymology,* St. Louis, Elsevier/Academic Press, 2006.
6. Ferrari G, Cusella-De Angelis G, Coletta M: Muscle regeneration by bone marrow-derived myogenic progenitors. *Science* 279: 1528–1530, 1998.
7. Caplan AI, Bruder SP: Mesenchymal stem cells: Building blocks for molecular medicine in the 21st century. *Trends Mol Med* 7: 259–264, 2001.
8. Friedenstein A, Kuralesova AI: Osteogenic precursor cells of bone marrow in radiation chimeras. *Transplantation* 12: 99–108, 1971.
9. Maniatopoulos C, Sodek J, Melcher AH: Bone formation in vitro by stromal cells obtained from bone marrow of young adult rats. *Cell Tissue Res* 254: 317–330, 1988.
10. Alhadlaq A, Mao JJ: Tissue-engineered neogenesis of human-shaped mandibular condyle from rat mesenchymal stem cells. *J Dent Res* 82: 951–956, 2003.
11. Warnke PH, Springer IN, Wiltfang J, *et al*: Growth and transplantation of a custom vascularised bone graft in a man. *Lancet* 364: 766–770, 2004.
12. Horwitz EM, Gordon PL, Koo WK, *et al*: Isolated allogeneic bone marrow-derived mesenchymal cells engraft and stimulate growth in children with osteogenesis imperfecta: Implications for cell therapy of bone. *Proc Natl Acad Sci U S A* 99: 8932–8937, 2002.
13. Yoon YS, Wecker A, Heyd L, *et al*: Clonally expanded novel multipotent stem cells from human bone marrow regenerate myocardium after myocardial infarction. *J Clin Invest* 115: 326–338, 2005.
14. Koc ON, Day J, Nieder M, *et al*: Allogeneic mesenchymal stem cell infusion for treatment of metachromatic leukodystrophy (MLD) and Hurler syndrome (MPS-IH). *Bone Marrow Transplant* 30: 215–222, 2002.
15. Rodriguez JP, Gonzalez M, Rios S, Cambiazo V: Cytoskeletal organization of human mesenchymal stem cells (MSC) changes during their osteogenic differentiation. *J Cell Biochem* 93: 721–731, 2004.
16. Stossel TP: On the crawling of animal cells. *Science* 260: 1086–1094, 1993.
17. Hayakawa K, Sato N, Obinata T: Dynamic reorientation of cultured cells and stress fibers under mechanical stress from periodic stretching. *Exp Cell Res* 268: 104–114, 2001.
18. Wakatsuki T, Schwab B, Thompson NC, Elson EL: Effects of cytochalasin D and latrunculin B on mechanical properties of cells. *J Cell Sci* 114: 1025–1036, 2001.
19. Rotsch C, Radmacher M: Drug-induced changes of cytoskeletal structure and mechanics in fibroblasts: An atomic force microscopy study. *Biophysics J* 78: 520–535, 2000.
20. Ohashi T, Ishii Y, Ishikawa Y, *et al*: Experimental and numerical analyses of local mechanical properties measured by atomic force microscopy for sheared endothelial cells. *Biomed Mater Eng* 12: 319–327, 2002.
21. Maniotis AJ, Chen CS, Ingber DE: Demonstration of mechanical connections between integrins, cytoskeletal filaments, and nucleoplasm that stabilize nuclear structure. *Proc Natl Acad Sci U S A* 94: 849–854, 1997.
22. Binnig G, Quate CF, Gerber C: Atomic force microscope. *Phys Rev Lett* 56: 930–933, 1986.
23. Radmacher M, Tillamnn RW, Fritz M, Gaub HE: From molecules to cells: imaging soft samples with the atomic force microscope. *Science* 257: 1900–1905, 1992.
24. Chang L, Kious T, Yorgancioglu M, *et al*: Cytoskeleton of living, unstained cells imaged by scanning force microscopy. *Biophys J* 64: 1282–1286, 1993.
25. Henderson E, Haydon PG, Sakaguchi DS: Actin filament dynamics in living glial cells imaged by atomic force microscopy. *Science* 257: 1944–1946, 1992.
26. Haga H, Sasaki M, Kawabata K, *et al*: Elasticity mapping of living fibroblasts by AFM and immunofluorescence observation of the cytoskeleton. *Ultramicroscopy* 82: 253–258, 2000.
27. Braet F, De Zanger R, Kalle W, *et al*: Comparative scanning, transmission and atomic force microscopy of the microtubular cytoskeleton in fenestrated liver endothelial cells. *Scanning Microsc Suppl* 10: 225–235, 1996.
28. Wu HW, Kuhn T, Moy VT: Mechanical properties of L929 cells measured by atomic force microscopy: Effects of anticytoskeletal drugs and membrane crosslinking. *Scanning* 20: 389–397, 1998.
29. Pavalko FM, Chen NX, Turner CH, *et al*: Fluid shear-induced mechanical signaling in MC3T3–E1 osteoblasts requires cytoskeleton-integrin interactions. *Am J Physiol* 275: C1591–C1601, 1998.
30. McGarry JG, Klein-Nulend J, Prendergast PJ: The effect of cy-

toskeletal disruption on pulsatile fluid flow-induced nitric oxide and prostaglandin E2 release in osteocytes and osteoblasts. *Biochem Biophys Res Commun* 330: 341–348, 2005.
31. Weinbaum S, Cowin SC, Zeng Y: A model for the excitation of osteocytes by mechanical loading-induced bone fluid shear stresses. *J Biomech* 27: 339–360, 1994.
32. Trickey WR, Vail TP, Guilak F: The role of the cytoskeleton in the viscoelastic properties of human articular chondrocytes. *J Orthop Res* 22: 131–139, 2004.
33. Brenner SL, Korn ED: Substoichiometric concentrations of cytochalasin D inhibit actin polymerization: Additional evidence for an F-actin treadmill. *J Biol Chem* 254: 9982–9985, 1979.
34. Mallein-Gerin F, Garrone R, van der RM: Proteoglycan and collagen synthesis are correlated with actin organization in dedifferentiating chondrocytes. *Eur J Cell Biol* 56: 364–373, 1991.
35. Spiegelman BM, Ginty CA: Fibronectin modulation of cell shape and lipogenic gene expression in 3T3-adipocytes. *Cell* 35: 657–66,1983.
36. Spiegelman BM, Farmer SR: Decreases in tubulin and actin gene expression prior to morphological differentiation of 3T3 adipocytes. *Cell* 29: 53–60, 1982.
37. McBeath R, Pirone DM, Nelson CM, *et al*: Cell shape, cytoskeletal tension, and RhoA regulate stem cell lineage commitment. *Dev Cell* 6: 483–495, 2004.
38. Salter DM, Robb JE, Wright MO: Electrophysiological responses of human bone cells to mechanical stimulation: evidence for specific integrin function in mechanotransduction. *J Bone Miner Res* 12: 1133–1141, 1997.
39. Lee HS, Millward-Sadler SJ, Wright MO, *et al*: Integrin and mechanosensitive ion channel-dependent tyrosine phosphorylation of focal adhesion proteins and beta-catenin in human articular chondrocytes after mechanical stimulation. *J Bone Miner Res* 15: 1501–1509, 2000.
40. Knight MM, Toyoda T, Lee DA, Bader DL: Mechanical compression and hydrostatic pressure induce reversible changes in actin cytoskeletal organisation in chondrocytes in agarose. *J Biomech* 39: 1547–1551, 2006.
41. Cunningham CC, Stossel TP, Kwiatkowski DJ: Enhanced motility in NIH 3T3 fibroblasts that overexpress gelsolin. *Science* 251: 1233–1236, 1991.
42. Cooper JA, Schafer DA: Control of actin assembly and disassembly at filament ends. *Curr Opin Cell Biol* 12: 97–103, 2000.
43. Chellaiah M, Hruska K: Osteopontin stimulates gelsolin-associated phosphoinositide levels and phosphatidylinositol triphosphate-hydroxyl kinase. *Mol Biol Cell* 7: 743–753, 1996.
44. Frank O, Heim M, Jakob M, *et al*: Real-time quantitative RT-PCR analysis of human bone marrow stromal cells during osteogenic differentiation in vitro. *J Cell Biochem* 85: 737–746, 2002.
45. Kasas S, Wang X, Hirling H, *et al*: Superficial and deep changes of cellular mechanical properties following cytoskeleton disassembly. *Cell Motil Cytoskeleton* 62: 124–132, 2005.
46. Rotsch C, Braet F, Wisse E, Radmacher M: AFM imaging and elasticity measurements on living rat liver macrophages. *Cell Biol Int* 21: 685–696, 1997.
47. Sato K, Nagayama K, Kataoka N, *et al*: Local mechanical properties measured by atomic force microscopy for cultured bovine endothelial cells exposed to shear stress. *J Biomech* 33: 127–135, 2000.